Image Simulation in Transmission Electron Microscopy

Earl J. Kirkland
Applied and Engineering Physics
Cornell University
Ithaca, N.Y. 14853

July 26, 2006

Abstract

This is a tutorial on scanning and fixed beam transmission electron microscope image simulation using the multislice method. It is the second in a series of lectures given in the summer school held at Cornell Univ. in the summer of 2006.

1 Introduction

Computer simulation of images has become a routine tool of high resolution transmission electron microscopy (conventional and scanning) of materials. This is a short tutorial on using the multislice method. For a more complete, formal discussion including detailed theory and a more complete list of references, see, for example, Kirkland[13] and the list of additional books given at the end. This presentation is less formal and gives some newer references and different examples. Also, this is the second of a series of lectures. It is assumed that the reader is familiar with the first lecture on linear imaging theory (Fourier transforms, transfer functions and point spread functions as in chap. 2,3,4 of Kirkland[13]).

2 Why do Image Simulations?

The resolution of high resolution conventional (CTEM) or scanning (STEM) transmission electron micrographs of materials are primarily limited by the aberrations of the lenses in the microscope and multiple scattering in the specimen. High resolution images of biological specimens are primarily limited by radiation damage, which is a different issue and will not be considered here.

Even for very thin specimens, the imaging electrons will likely interact strongly enough with the specimen to be scattered more than once while traveling through the specimen. This multiple scattering (also called dynamical scattering) may influence the image in unexpected ways such that the image is no longer related to the specimen structure in an simple manner. The goal of image simulation is to understand this image structure better. In summary the main goals of image simulation are:

understanding: Image simulation may help to understand the detailed structure in the image to separate what is due to the specimen, what is due to the instrument and help unravel the effects of multiple scattering.

improvement: Image simulation may help to understand how the image is formed and generate intuition on ways to improve the image and instrumentation.

3 Relativity and Quantum Mechanics

The electron energies used in the electron microscope are typically large enough to produce electron velocities that are a significant fraction of the speed of light c. For example a 200 keV electron is traveling at about half the speed of light. This high energy produces some changes in the electron properties as compared to its low energy non-relativistic properties. The electron velocity, mass and wavelength are shown in fig. 1. The electron velocity and mass are significantly altered by relativity. Please refer to chp. 2 of Kirkland[13] for the relevant equations.

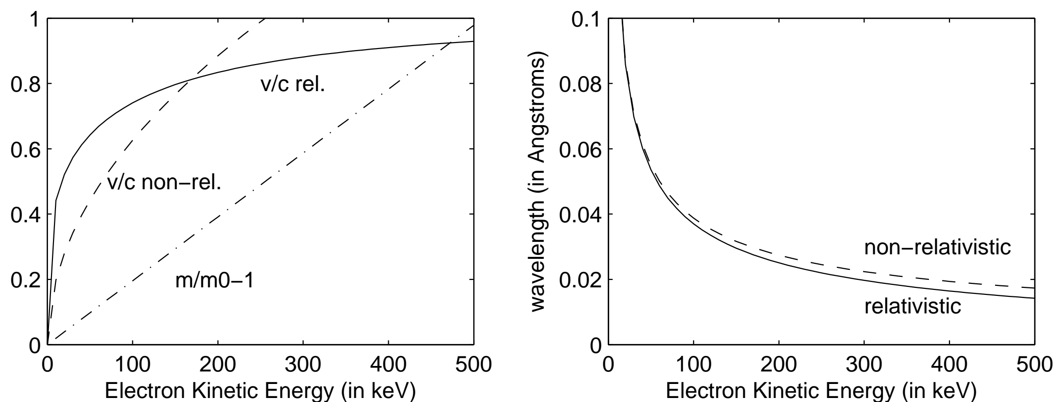

Figure 1: Relativistic properties of the electron. The velocity v relative to the speed of light c (in vacuum) is on the left and the wavelength is on the right. Both non-relativistic and relativistic values are shown. The ratio of the relativistic mass m to the rest mass m_0 of the electron is also shown on the left.

In the electron microscope the electron beam has a typical energy in the range 100 keV to 1 Mev. Typical potentials in the specimen are usually much less, in the range 10 eV to 1000 eV, so the incident electrons pass through the specimen with a relatively small change.

On the atomic scale, the behavior of the electron is governed by its quantum mechanical wave nature as described by the Schrödinger equation:

$$\left[-\frac{\hbar^2}{2m}\nabla^2 - eV(\vec{x})\right]\psi(\vec{x}) = E\psi(\vec{x}) \tag{1}$$

where $\psi(\vec{x})$ is the wave function of the electron at position $\vec{x}$, $\hbar = h/2\pi$ is Planck's constant divided by 2π, m is the mass of the electron, $e = |e|$ is the magnitude of the charge of the electron, E is the total energy of the electron and $-eV(\vec{x})$ is the potential energy of the electron.

The Schrödinger equation is not relativistically correct. The Dirac wave equation is relativistically correct and properly predicts the electron spin and the existence of the positron, but however is more difficult to deal with mathematically. An approximate compromise of using the Schrödinger equation with the relativistic electron mass and wavelength is usually adequate for the medium energies typically used in the electron microscope (Fujiwara[4]), and will be used here.

4 The Transmission Electron Microscope

There are two fundamental forms of a transmission electron microscope (TEM) as is illustrated in a simplified schematic form in fig. 2. In the conventional or fixed beam form (CTEM) the specimen is illuminated by

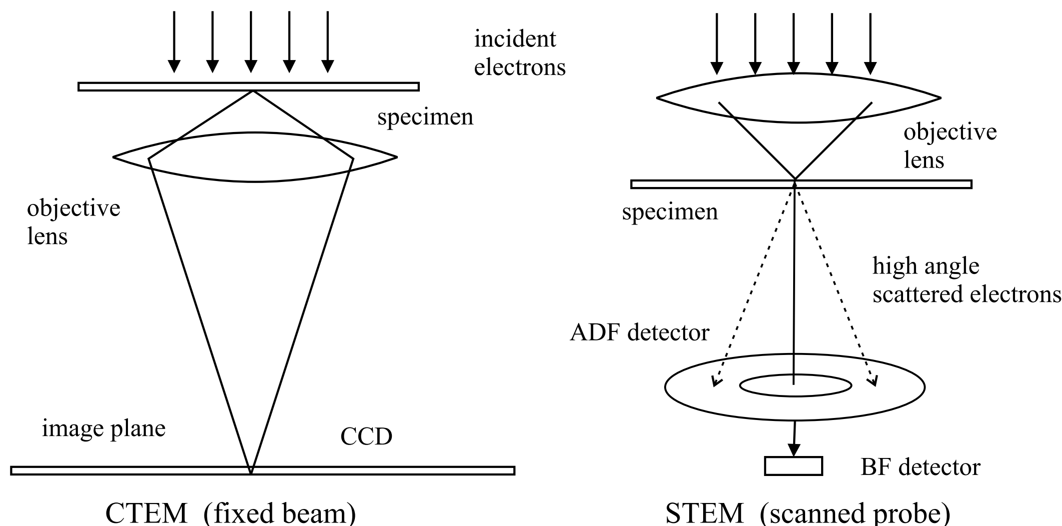

Figure 2: Simplified schematic of the Conventional Transmission Electron Microscope (CTEM, left) and the Scanning Transmission Electron Microscope (STEM, right). Neither drawing is to scale.

a parallel (or nearly so) beam of electrons. An objective lens forms an image of the specimen in parallel with a fixed beam similar to a standard light optical microscope. The bright field image is typically phase contrast. In the scanning form (STEM) a small focused probe (of order 1 to 2 Å in diameter) is scanned across the specimen in raster form. The transmitted electrons that have been scattered to large angles form an annular dark field (ADF) image that has a strong dependence on the atomic number of the atoms in the specimen (Z-contrast). The transmitted electrons that are on the optic axis (nearly unscattered) form the bright field (BF) image which exhibits phase contrast similar to CTEM (if set up correctly).

Generally speaking, bright field (BF) CTEM has a strong signal but lower resolution and more ambiguity in the image. ADF-STEM has higher resolution and a more direct (less ambiguous) relationship to the specimen but a smaller signal.

5 Numerical (Computer) Calculations for Thick Specimens

Electrons interact strongly enough with the specimen that ”thick” means more than a few Angstroms for most materials. In most case the electrons will undergo multiple (or dynamical) scattering as they pass through the specimen. This section will discuss the propagation of the electrons through the specimen and the next section will add instrumental effects such as lens aberrations. There are two principle means of calculating a transmission electron microscope image (scanning or conventional), the Bloch wave method and the multislice method.

Bloch wave: The electron wave function is expanded in Bloch waves inside a crystalline specimen, which have the periodicity of the specimen and satisfy the Schrödinger equation. Requires finding the Eigenvectors and values of a large matrix. Good for small perfect crystals but the computer time scales as N^3 where N is the number of Bloch waves or Fourier components (N increases with resolution).

multislice: Divide the specimen into many thin slices. Alternately transmit and propagate the slowly varying portion of the wave function through the specimen. Will work on crystalline or nearly amorphous specimens. Using an efficient fast Fourier transform (FFT) the computer time scales approx. as $N \log(N)$ where N is the number of Fourier components (N increases with resolution).

The Bloch wave approach is described in several books (for example, DeGraf[7]) and will not be discussed in detail here. The multislice method was first described by Cowley and Moodie[2] and later expanded by Goodman and Moodie[6]. The fast Fourier transform (FFT) was first added by Ishzuka and Uyeda[9] and Bursill and Wilson[1] and greatly improves the computational efficiency (reduces CPU time) of the multislice method. The FFT based multislice method is presented in Kirkland[13] and will be discussed briefly below.

The wavelength of a 200 keV electron is λ= 0.025 Å. A straightforward numerical sampling of this wavelength would require of order 10 points per wavelength. To sample a small specimen in a cube of 100 Åper side would require about $(100/0.0025)^3$ or 6.3×10^{13} points. Even in single precision (four bytes per value) this would require 2.4×10^5 Gbytes of memory, which is clearly not possible in the near future. Clearly some other approach must be found. The Bloch wave method solves this problem by expanding in a small basis set plane waves so real space sampling is not really used. However there is still a finite sample in reciprocal space.

5.1 Multislice

The multislice method solves this sampling problem by factoring the electron wave function into a part that varies with the wavelength and a slowly varying portion that is sampled in real space at a much larger sample spacing (because the specimen has only a small effect on the scale of the electron wavelength). The full electron wave function ψ_f traveling in the positive z direction is:

$$\psi_f = \psi \exp(2\pi i z/\lambda) \tag{2}$$

where λ is the electron wavelength and ψ is the slowly varying portion of the wave function. Insert this expression for ψ_f into the Schrödinger equation and solve for the slowly varying portion of the wave function ψ. Now the sampling of the slowly varying portion may be spaced many wavelengths apart. This approximation is justified because the incident electron beam is a relatively high energy and is not changed significantly on the scale of its wavelength. The possibility of back scattered waves will also be neglected.

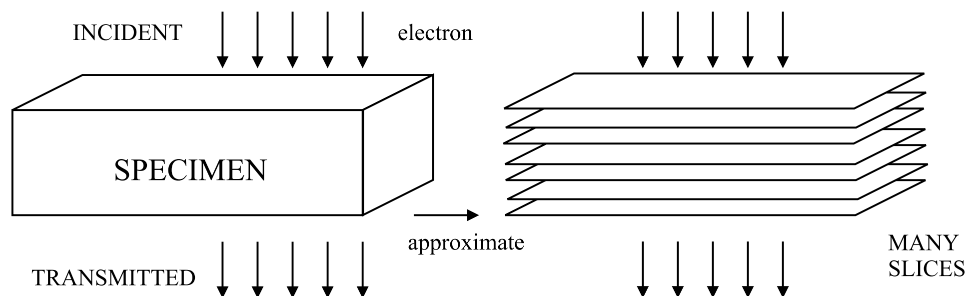

Figure 3: The multislice approximation converts a specimen (left) into many thin slices (right). The electron wave is incident on the top of the specimen, is transmitted through the specimen and exits on the bottom. Each slice (of the specimen) is thin enough to be approximated as a simple phase shift of the electron wave which is propagated between slices as a free space wave.

The second approximation in the multislice method is the actual slicing of the specimen as in fig. 3. The specimen is sliced up much like a loaf of bread. The incident wave enters the specimen at the top, propagates through the specimen and exits at the bottom. In CTEM the incident wave is a uniform plane wave and in STEM the incident wave is a small focused probe (at each position in the image). The specimen is divided into many slices, each of which is thin enough to be approximated as a simple phase shift of the electron beam. The electron beam propagates between slices as a small angle outgoing wave (Fresnel diffraction). The wave is transmitted through a slice of thickness Δz and then propagates a distance Δz to the next layer.

With some mathematical manipulation of the slowly varying portion of the electron wave function in the

Schrödinger equation and dropping small terms yields the following for the multislice equation:

$$\psi(x, y, z + \Delta z) = p(x, y, \Delta z) \otimes [t(x, y, z)\psi(x, y, z)] + \mathcal{O}(\Delta z^2) \tag{3}$$

where $\otimes$ represents convolution and Δz is a small slice of the specimen along the beam direction. The transmission function for the portion of the specimen between z and $z + \Delta z$ is:

$$t(x, y, z) = \exp\left[i\sigma \int_z^{z+\Delta z} V(x, y, z')dz'\right] \tag{4}$$

where $\sigma = 2\pi m e\lambda/h^2$ is the interaction parameter, and $V(x, y, z)$ is the potential due to the atoms inside the specimen (calculated from relativistic Hartree-Fock for isolated atoms). The propagator function $p(x, y, z)$ and its Fourier transform $P(k)$ are:

$$\begin{aligned} P(k, \Delta z) &= \exp\left(-i\pi\lambda k^2 \Delta z\right) \\ p(x, y, \Delta z) &= FT^{-1}\left[P(k, \Delta z)\right] = \frac{1}{i\lambda\Delta z} \exp\left[\frac{i\pi}{\lambda\Delta z}(x^2 + y^2)\right] \end{aligned} \tag{5}$$

which is equivalent to Fresnel diffraction (near field) for a distance Δz. If each slice of the specimen is labeled with subscript n ($z = n\Delta z$) then the multislice equation becomes:

$$\psi_{n+1}(x, y) = p_n(x, y, \Delta z_n) \otimes [t_n(x, y)\psi_n(x, y)] + \mathcal{O}(\Delta z^2) \tag{6}$$

Convolution scales as N^2 where N is the number of points and is still a very time consuming calculation on the computer. However, this form of the equation is very well suited for use of the Fast Fourier Transform or FFT, which is a highly efficient well developed numerical algorithm. The CPU time for the FFT scales as $N \log(N)$. Using the FFT, signified as FT:

$$\psi_{n+1}(x, y) = FT^{-1}\left\{P_n(k_x, k_y, \Delta z_n)FT\left[t_n(x, y)\psi_n(x, y)\right]\right\} + \mathcal{O}(\Delta z^2) \tag{7}$$

The multislice method reduces to a succession of transmit and propagate operations with a fast Fourier transform in between each which is summarized in fig. 4.

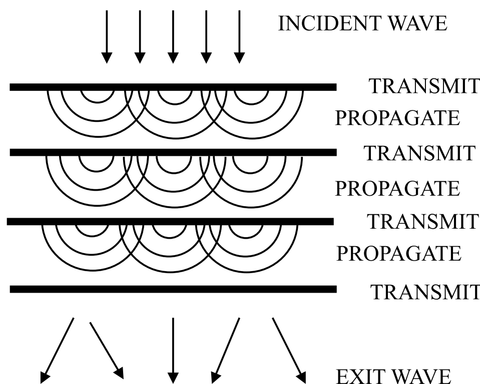

Figure 4: The multislice method successively transmits the electron wave through each slice and then propagates it to the next slice. The incident wave is a plane wave for CTEM (shown) and a focused probe for STEM (not shown).

5.2 Instrumental Effects (Lens Aberrations)

The image in both the CTEM and the STEM is strongly affected by the aberrations in the objective lens. This is the topic of the previous lecture and is covered in more detail in chp. 3 and 5 of Kirkland[13], and is summarized here.

In the CTEM the incident wave is a uniform plane wave which is transmitted through the specimen (multislice calculation). The electron wave function exiting the crystal $\psi_T(\vec{x})$ is imaged by the objective lens onto the CCD image detector. In practice there are several projector lens after the objective but these can be ignored because the effects of the objective lens have been greatly magnified. The aberrations (mainly spherical and defocus) influence the image as:

$$g(\vec{x}) = |\psi_T(\vec{x}) \otimes h(\vec{x})|^2 \quad (8)$$
$$= |FT^{-1}[\Psi_T(\vec{k})H(\vec{k})|^2 \quad (9)$$

where $h(\vec{x})$ is the point spread function of the objective lens. $\vec{x}$ is the position in the image and $\vec{k}$ is the spatial frequency vector conjugate to $\vec{x}$. $\Psi_T(\vec{k})$ is the Fourier transform of $\psi_T(\vec{x})$. The convolution is more efficiently done as an FFT and the Fourier transform of the point spread function, also known at the transfer function is:

$$H(\vec{k}) = \exp[-i\chi(\vec{k})] \quad (10)$$
$$\chi(\vec{k}) = \frac{2\pi}{\lambda}\left[\frac{1}{4}C_s\lambda^4k^4 - \frac{1}{2}\Delta f\lambda^2k^2\right] \quad (11)$$

where C_s is the coefficient of spherical aberration (third order), and Δf is defocus

In the STEM the lens is before the specimen not after as in the CTEM. The objective lens forms a small focused probe incident on the specimen which is scanned across the specimen. The wave function of the probe is calculated as:

$$\psi_P(\vec{x}, \vec{x}_P) = A_P \int_{apert} \exp[-i\chi(\vec{k}) - 2\pi i\vec{k}\cdot(\vec{x} - \vec{x}_P)]d\vec{k} \quad (12)$$

where $\vec{x}_P$ is the position of the probe and the integral is over the objective aperture. The leading constant A_p is chosen to normalize the total integrated intensity (usually to unity). Generally speaking the optimum aperture and defocus are the Scherzer conditions:

$$\Delta f_{opt} = \sqrt{1.5C_s\lambda} \quad (13)$$
$$\alpha_{max} = \left(\frac{6\lambda}{C_s}\right)^{1/4} \quad (14)$$

where α is the semi-angle of the electron rays in the lens (objective aperture size). The optimum conditions for ADF-STEM are usually slightly smaller values for both, $\Delta f \sim \sqrt{C_s\lambda}$ and $\alpha_{max} \sim (4\lambda/C_s)^{1/4}$. The resolution in BF-CTEM is approx. $0.7(C_s\lambda^3)^{1/4}$ and the resolution in ADF-STEM (probe size) is approx. $0.43(C_s\lambda^3)^{1/4}$. See Kirkland[13] for a more detailed discussion of astigmatism and partial coherence in BF-CTEM.

6 What Can Go Wrong

There are a large number of things that can go wrong in an image simulation. The proposed specimen structure must be specified in some detail, usually in the form of a list of atomic coordinates and atomic numbers in a unit cell. Even less well known is the thickness of the specimen. Usually a large sequence of possible specimen thicknesses are calculated and compared to experiment.

The instrumental (optical) parameters such as the aberration constants (C_s, etc.) and aperture size of the objective lens and lens defocus must be known. Usually defocus is not know very well (particularly in bright field phase contrast). Frequently a *defocus series* is calculated for comparison to experiment. There are also a variety of parameters such as defocus spread, illumination angle etc. that are hard to estimate but can influence the image (see Kirkland[13] for more details).

There are also many parameters that are solely related to the calculation and have very little to do with the microscope or specimen but can dramatically affect the calculation. These parameters include the sampling size (pixel size) in the image and slices and the slice thickness itself.

Multislice almost always uses an FFT to reduce the total CPU time. The FFT is a discrete Fourier transform which repeats the image infinitely in all directions. Although the image is only displayed as a single image you should remember that it is really an infinite array of identical side-by-side images. This produces a strange effect called the *wrap-around error*. The left side of the image in essence touches the right side of the image (and vice versa) and the top of the image touches the bottom of the image (see fig. 6.10 and 6.11 in Kirkland[13]). To use the FFT each image and slice must obey periodic boundary conditions or be an integer number unit cells of the specimen (called a super cell). Interfaces and defects must be imbedded inside a large super cell (brief discussion in section 6.8 of Kirkland[13]).

In summary, some of the things that need to be specified correctly are:

specimen parameters: atomic coordinates and numbers of the specimen and thickness of specimen

instrumental parameters: defocus, C_s, objective aperture, etc.

sampling size: number of pixels in the image and slice and the slice thickness. Ensure that the total integrated intensity is at least 0.9 or higher (1.0 to start). Calculations with slightly higher or lower sampling should yield the same result if the sampling is adequate.

slice thickness: usually the slices should correspond to the existing atomic layers in the specimen. If the slices are too thick then the total integrated intensity will decline too much (as in the sampling size issue) and may produce false high order Laue zones corresponding to the slice thickness.

wrap-around error: each slice must obey periodic boundary conditions

7 Programs

There are a variety of image calculation programs in existence. Many have been written for private use only. Some have been made available commercially for varying amounts of money and some are available as a free download. A partial list of some programs is shown in table 1.

program	author	year	type	comments
SHRLI	O'Keefe and Buseck[14]	1978,9	M	
TEMPAS	Kilaas[11]	1987	M	
EMS	Stadelmann[19]	1987	B	
NCEMSS	O'Keefe and Kilaas[15]	1988	M	
MacTEMPAS	Kilaas[12]	?	M	on-line
TEMSIM	Kirkland[13]	1998	M	on CD
?	Ishizuka[8]	2001	B, M	online
?	deGraf[7]	2003	B	online
JEMS	Stadelmann[20]	2004	B, M	online
WebEMAPS	Zuo[18]	2005	B	online

Table 1: Some image simulation software packages appearing in the literature or on-line. Type M is multislice and type B is Bloch-Wave. Some of the listed programs may be commercial. Many other private programs likely exist.

8 Examples

Silicon is a technologically important material and is well known to many people. When viewed down the 110 direction, groups of atoms are far enough apart to be visible in many microscopes currently available. The structure of the three main projections of silicon are summarized in fig. 5.15 (and fig. 7.1 for 110 GaAs) of Kirkland[13]. The 110 projection has pairs of atoms spaced 1.4Å apart (the so-called dumb-bells) and these pairs are repeated at roughly 3.1Å intervals. The unit cell size is 3.8Å×5.4Å in the image plane and 3.8Å along the beam direction. The unit cell divides easily into two layers each 1.9Å thick. The easiest approach to programming multislice using an FFT is too require the unit cell to be rectangular because the 2D FFT is decomposed into successive 1D FFT's along each direction. This projection of silicon is conveniently rectangular. Most non-rectangular unit cells can be converted to an equivalent rectangular unit cell by taking a larger volume (see discussion in chp. 7 of Kirkland[13]).

Silicon is a good place to start to learn how to do a multislice image calculation because it has a simple unit cell and low atomic number atoms. High atomic number atoms or high density atoms usually require a much high sampling (more pixels and much more computer time). Silicon can be done with a relatively small number of pixels with only a small amount computer time. This example will use the programs given in Kirkland[13]. The programs are written with a simple command line interface so they can be run on different machines (no specific machine dependencies). The lack of a fancy graphical user interface may not be pleasant but it makes the programs easily portable.

First generate a description of the specimen. There are two different layers, and there should be a text file with the atomic coordinates for each layer (two files). The input file for the first layer is:

```
  3.8396  5.4300  1.9198
 0
14
  1.0000  0.0000  0.0000
  1.0000  0.5000  0.7500
```

The input file format is described in detail on pg. 164 of Kirkland[13]. The first line is the unit cell size (in Å). The second line is the number of symmetry operations (none here) to apply to the following coordinates (not listed). The last three lines are the atomic number followed by the coordinates for this atomic number. The first number on each line is the occupancy (1.0 in this case) followed by the coordinates relative to the unit cell size. There can many different atomic numbers each with its own set of coordinates. There should be two blank lines at the end of the file. The second layer is described in a similar manner as:

```
  3.8396  5.4300  1.9198
 0
14
  1.0000  0.0000  0.2500
  1.0000  0.5000  0.5000
```

Next the program *atompot* is run for each of this input files to produce a binary (TIFF format) file containing the projected atomic potential of each of these layers. This program allows the unit cell to be expanded an integer number of times in each direction and allows the user to specify the number of pixels (sampling). In practice you need to do a sequence of runs to determine the proper sampling (number of pixels and number of unit cells) that produce good results as described in section 7.1 of Kirkland[13] for gallium arsenide. Silicon is a light atom and only requires a modest sampling. It has been found that 6×4 unit cells of 256×256 pixels works reasonably well for BF-CTEM of this specimen.

8.1 BF-CTEM

The program *mulslice* takes these potentials as input to run the multislice algorithm itself. The total specimen is specified as the layer repeat structure. For example, 100Å of this specimen is specified as 26(ab) meaning 26 repeats of (ab) to give ababab... The result for this thickness is shown in fig. 5. This is the wave function of the electrons exiting the bottom of the specimen (in fig. 3).

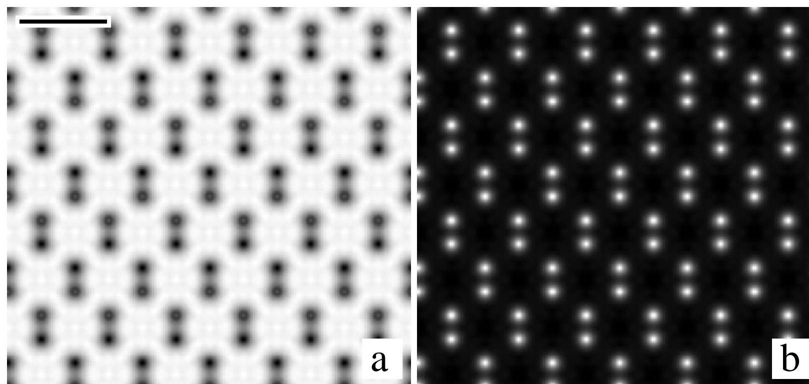

Figure 5: The wave function (200 keV) transmitted through 100 Å of 110 silicon calculated using the multislice method. The real part is on the left and the imaginary part is on the right. Silicon atoms are dark in the real part and white in the imaginary part (contrast may vary with thickness). The scale bar is 5 Å.

The results of *mulslice* are next feed into the program *image* to generate images with different defocus. The programs are separated so that a single result of multislice can be used many different times to generate several different images with different defocus values. Typically *image* is much quicker than *mulslice*.

The results of applying *image* to the *mulslice* results are shown in fig. 6. Each row is a different specimen thickness (a different run of *mulslice*) and each col. is a different defocus value (one run of *mulslice* per row and one run of *image* per image). Each image also includes the effects of partial coherence with an illumination angle 1 mrad and defocus spread of 100Å (theory described in Kirkland[13]). An objective aperture larger than optimum (15 mrad instead of 12 mrad) was used as is common in practice because the partial coherence effect tend to produce a virtual aperture. Defocus values were chosen as $\Delta f = \sqrt{(2n - 0.5)C_s\lambda}$ for $n = 1, 2, 3....$ n=1 is the Scherzer condition and other integer values have some interesting properties (see section 3.1 of Kirkland[13]). This calculation took just a min. or two on a standard desktop computer.

There are several interesting effects in fig. 6. Both defocus and thickness influence the image. In particular there is a contrast reversal at the thickest specimen (bottom row). In bright field phase contrast each atom should be dark on a white background. However the situation has reversed in the thick specimen.

8.2 ADF-STEM

ADF-STEM takes significantly more computer time for two reasons. A multisilce calculation must be performed at each position of the probe, and the ADF detector typically extends to very high angles which need to be calculated (much higher sampling or more pixels). It is sometimes easier to figure out the input files using CTEM (as in the previous section) and then switch to STEM. The program *stemslic* takes the same input files as *mulslice* (both from *atompot*).

Because of the large computer time requirements *stemslic* can produce simple line scans instead of images which run faster. Also the atomic potentials, and electron wave function do not have to have the same number

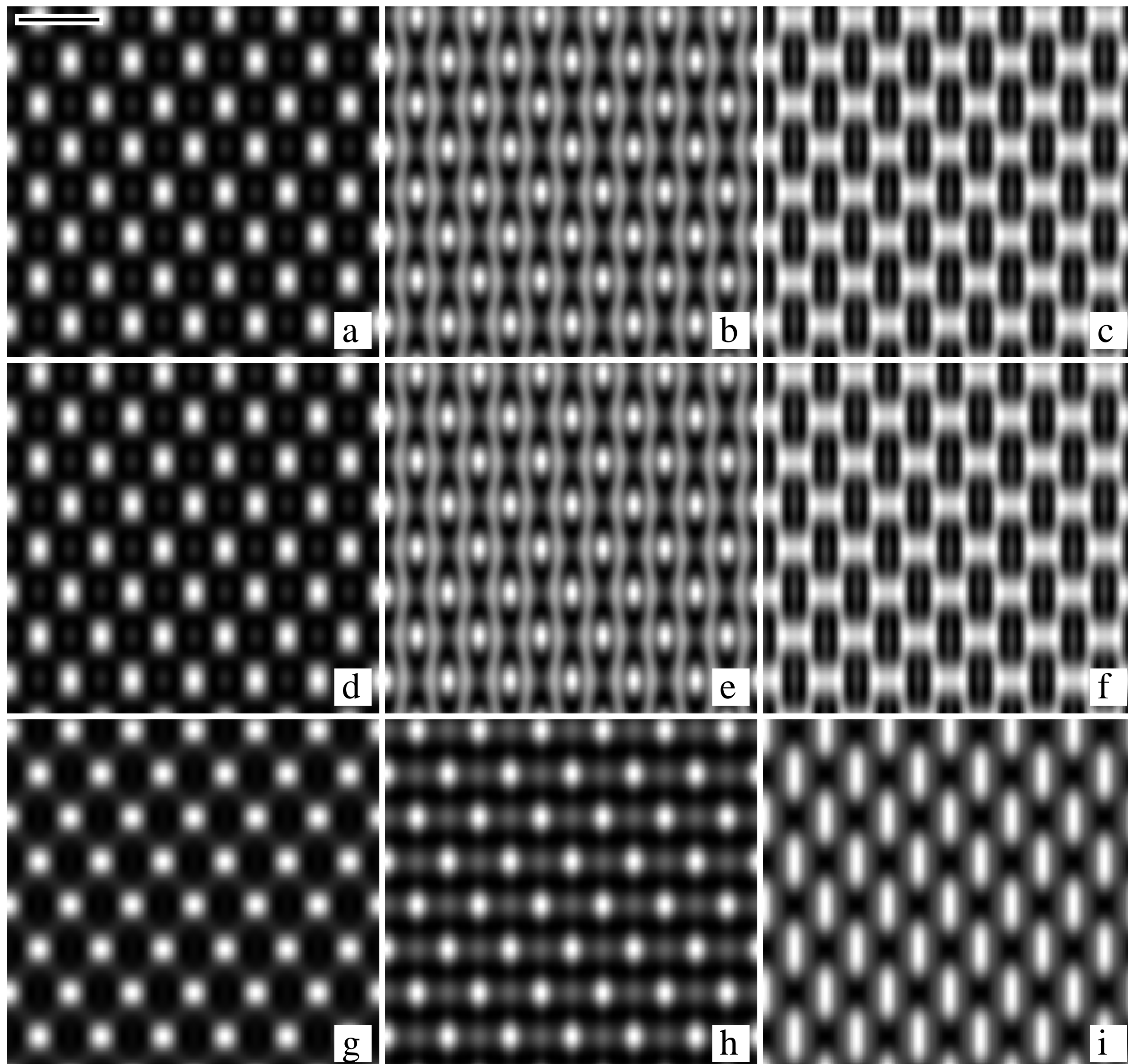

Figure 6: BF-CTEM images calculated for 110 silicon using the multislice method for 200 keV electrons with C_s= 0,7 mm. Specimen thickness increase from top to bottom and defocus increases from left to right. Thickness is: a,b,c) 50Å, d,e,f) 100Å, g,h,i) 200Å. Defocus is: a,d,g) 513Å, b,e,h) 983Å, c,f,i) 1291Å. The scale bar is 5 Å.

of pixels and only a small portion of the available size need be calculated.

The optical parameters for an optimum (smallest) probe are $\Delta f = \sqrt{C_s \lambda} \sim 400$Å, and $\alpha_{max} \sim 11$ mrad. Section 7.1 of Kirkland[13] tests the sampling requirements for 110 GaAs. Because silicon is a lighter atom, these requirements should also satisfy silicon, which will be modeled as 6 by 4 units cells (in the supercell). Usually you should repeat the procedure in section 7.1 for each new specimen. The ADF detector typically extends to very high angles which also requires high sampling. With 512×512 pixels the maximum scattering angle is about 186 mrad. (for this supercell size and electron wavelength) which will be sufficient (200 mrad might be better but would require more computer time).

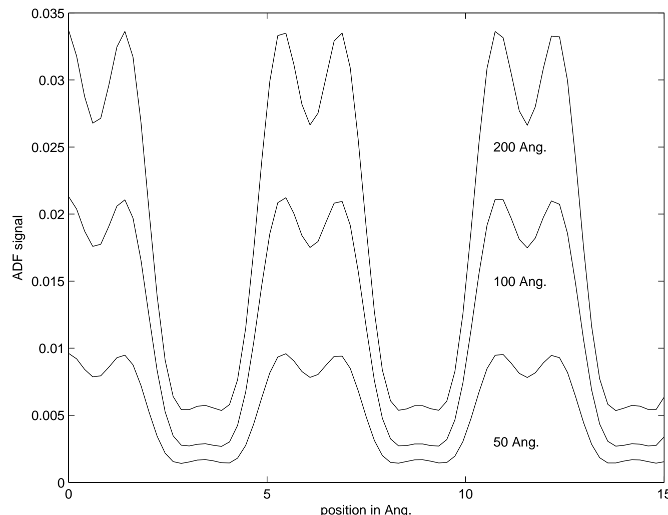

Figure 7: ADF-STEM line scan calculated for 110 silicon using 200 keV, C_s= 0.7mm, Δf= 400Å, obj. aperture 11 mrad. The scan is along a col. parallel to the silicon dumbbells for three different thickness (shown).

Fig. 7 shows the results of running *stemslic* as a line scan along a col. parallel to the silicon dumbbells (close pairs of atoms). The projected atomic potentials calculated by *atompot* as described in the previous section on BF-CTEM were used (but with more pixels, higher sampling). These optical parameter should produce a probe size of about 1.4Å, so the silicon atom pairs should just be resolved, which they are. The ADF signal increases nearly linearly with thickness unlike BF which has reversed contrast. The signal from 100Å thickness is about twice that of 50Å thickness, however the signal from 200Å thickness is not quit twice that of 100Å thickness. ADF-STEM is much closer to the actual structure in the specimen, but still has a few small nonlinearities that must be understood. Heavier atoms or thicker specimens will have more nonlinear feature in both BF and ADF (BF is always more of a problem in this respect).

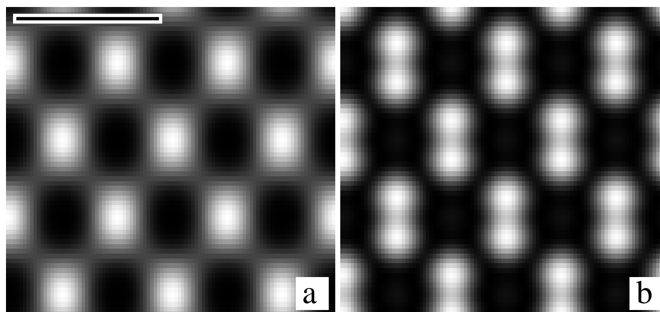

Figure 8: STEM images calculated for 110 silicon (50 Å thick) using 200 keV, C_s= 0.7mm, Δf= 400Å, obj. aperture 11 mrad. The BF image (detector angles 0 to 1 mrad) is shown on the left and the ADF image (detector angles 40 to 150 mrad) is shown on the right. Atoms should be black in BF and white in ADF. One unit cell of 32 by 32 pixels was calculated and expanded to several unit cells as shown. This took about 40 min. of computer time. The scale bar is 5 Å.

Fig. 8 show an ADF-STEM image of 110 silicon. Only the thinnest specimen was calculated to limit the computer time. Several different detector geometries can be run at the same time with no significant increase in computer time. The BF image (on left) should be nearly identical to the image in CTEM (which

it is) by the reciprocity theorem. The ADF image (on right) illustrates that the silicon atom pairs are just barely resolved as expected.

9 Exercises

[1] Repeat the above calculations for BF-CTEM images of 110 silicon (some portion of fig. 6). Try one or more thickness and defocus values. If time permits, compare the images to what you get with a Scherzer aperture size of 12 mrad. Some of these images may exhibit frequency doubling where the lattice spacing becomes half its expected value (this is due to a complicated interference of Fourier component of the image that have been phase shifted in a nonlinear manner by the specimen and objective lens).

[2] Repeat one of the above line scans for ADF-STEM of 110 silicon.

[3] Try to calculate the image of an edge of a thin (50 to 100Å) silicon 110 crystal with a single heavy (dopant) atom on the exit surface in the crystalline portion. The edge of the crystal should show a Fresnel fringe in BF but not in ADF, and the heavy atom should be visible in ADF but not in BF. You have to create a long narrow unit cell that is half filled with silicon and use *atompot* to expand in only one direction. There should be three potential files all together, two for silicon and one for the single heavy atom (must exactly match the size of the silicon unit cell). To keep the computer time to something that is reasonable only use a thin crystal and do only a line scan in ADF-STEM (be careful to hit the center of the single heavy atom).

10 Further Reading

Below is a list of some books on transmission electron microscopy that might be of interest. It is not comprehensive and there may be many worthwhile books that have been left out (apologies to the authors). This is just a starting point.

Some Recent Books on Electron Microscopy

1. M. De Graf, *Intro. to Conventional Transmission Electron Microscopy*, Cambridge Univ. Press, 2003[7]
2. J. W. Edington, *Practical Electron Microscopy in Materials Science*, Van Nostrand Reinhold, 1976[3]
3. B. Fultz and J. Howe, *Transmission Electron Microscopy and Diffractometry of Materials*, Springer, 2001[5]
4. R. Keyse et al, *Intro. to Scanning Transmission Electron Microscopy*, Springer, 1998[10]
5. E. J. Kirkland, *Advanced Computing in Electron Microscopy*, Plenum, 1998[13]
6. L. Reimer, *Transmission Electron Microscopy, third edition*, Springer-Verlag, 1993[16]
7. J. C. H. Spence, *Experimental High-Resolution Electron Microscopy*, Oxford University Press, 2003[17]
8. J. C. H. Spence and J. M. Zuo, *Electron Microdiffraction*, Plenum Press, 1992[18]
9. D. B. Williams and C. B. Carter, *Transmission Electron Microscopy, A Textbook for Materials Science*, Plenum Press, 1996[21]

11 Acknowledgements

This summer school has been sponsored by the Kavli Institute for Nanoscale Science and the School of Applied and Engineering Physics at Cornell Univ. Thanks are due to L. Fitting, S. Maccagnano, K. A. Mkhoyan and P. Ercius for help with proofreading.

References

[1] L. A. Bursill and A. R. Wilson. Electron-optical imaging of the hollandite structure at 3 å resolution. *Acta Cryst.*, A33:672–676, 1977.

[2] J. M. Cowley and A. F. Moodie. The scattering of electrons by atoms and crystals. I. a new theoretical approach. *Acta Cryst.*, 10:609–619, 1957.

[3] J. W. Edington. *Practical Electron Microscopy in Materials Science.* Van Nostrand Reinhold, New York, 1976.

[4] K. Fujiwara. Relativistic dynamical theory of electron diffraction. *J. Physical Society of Japan*, 16:2226–2238, 1961.

[5] B. Fultz and J. Howe. *Transmission Electron Microscopy and Diffractometry of Materials.* Springer, Berlin, 2001.

[6] P. Goodman and A. F. Moodie. Numerical evaluation of N-beam wave functions in electron scattering by the multislice method. *Acta Cryst.*, A30:280–290, 1974.

[7] M. De Graf. *Intro. to Conventional Transmission Electron Microscopy.* Cambridge Univ. Press, Cambridge, UK, 2003.

[8] K. Ishizuka, 2006. www.hremresearch.com.

[9] K. Ishizuka and N. Uyeda. A new theoretical and practical approach to the multislice method. *Acta Cryst.*, A33:740–749, 1977.

[10] R. J. Keyse, A. J. Garrett-Reed, P. J. Goodhew, and G. W. Lorimer. *Intro. to Scanning Transmission Electron Microscopy.* Springer, New York, 1998.

[11] R. Kilaas. Interactive simulation of high-resolution electron micrographs. In G. W. Bailey, editor, *Proceedings of the 45th Annual Meeting of the Microscopy Society of America*, pages 66–69. San Fransisco Press, 1987.

[12] R. Kilaas, 2006. www.totalresolution.com/index.html.

[13] E. J. Kirkland. *Advanced Computing in Electron Microscopy.* Plenum, New York, 1998.

[14] M. A. O'Keefe and P. R. Buseck. Computation of high resolution TEM images of materials. *Trans. American Crystallography Assoc.*, 15:27–46, 1979.

[15] M. A. O'Keefe and R. Kilaas. Advances in high-resolution image simulation. In P. W. Hawkes, F. P. Ottensmeyer, W. O. Saxton, and A. Rosenfeld, editors, *Image and Signal Processing in Electron Microscopy, Scanning Microscopy, Supplement 2*, pages 225–244, Chicago, 1988. Scanning Microscopy Intern.

[16] L. Reimer. *Transmission Electron Microscopy*, volume 36 of *Spring Series in Optical Sciences.* Springer-Verlag, New York, third edition, 1993.

[17] J. C. H. Spence. *Experimental High-Resolution Electron Microscopy.* Oxford University Press, New York, 3 edition, 2003.

[18] J. C. H. Spence and J. M. Zuo. *Electron Microdiffraction.* Plenum Press, New York, 1992. emaps.mrl.uiuc.edu.

[19] P. A. Stadelmann. EMS - a software package for electron diffraction analysis and HREM image simulation in materials science. *Ultramicroscopy*, 21:131–146, 1987.

[20] P. A. Stadelmann. JEMS - EMS java version, 2004. cimewww.epfl.ch/people/stadelmann.

[21] D. B. Williams and C. B. Carter. *Transmission Electron Microscopy, A Textbook for Materials Science.* Plenum Press, New York, 1996.